

Using Speckle Images for Determining the Local Plastic Strains Arising at High-Cycle Fatigue of 09G2S Steel

A. P. Vladimirov^{a,b*}, N. A. Drukarenko^a, and K. E. Myznov^b

^a Institute of Engineering Science, Ural Branch, Russian Academy of Sciences, Yekaterinburg, 620049 Russia

^b Ural Federal University, Yekaterinburg, 620002 Russia

*e-mail: vap52@bk.ru

Received March 4, 2021; revised April 16, 2021; accepted May 4, 2021

Abstract—Plastic strains arising in the zone of fatigue crack initiation are estimated with the aid of time-averaged speckle images on a sample of 09G2S steel with two grooves 2.5 mm in radius. It is shown that the fatigue fracture appears owing to localization of irreversible processes in the region less than 1 mm and the limit value of tension plastic strains is on the order of 10^{-1} . As an indication of fracture, it is proposed to use the fact that the normed temporal autocorrelation function of radiation intensity reduces to a negative value.

Keywords: speckles, image, high-cycle fatigue, deformation, fracture.

DOI: 10.1134/S1063785021080137

The study of high-cycle fatigue is enjoying interest at present due to the fact that 50–70% of engineering parts are destroyed by this type of fatigue [1–3]. Despite a long history of study [4–6] and multiple publications [7, 8], there are today no nondestructive inspection methods and no methods for estimating residual life of parts operating under high-cycle fatigue conditions, which could satisfy the requirements of the engineering practice [2]. Directly after the invention of lasers and discovery of speckle structure of scattered radiation, specklograms and holograms were used to study fatigue phenomena [9–11]. However, they have not received widespread application owing to nonmonotonic variation in the registered signals and labor intensity of techniques. The above-mentioned disadvantages of speckle and holographic methods were overcome in [12–14], and the authors of [13] provided a theoretical justification for the method of time-averaged speckle images (speckle patterns in the plane of object image), demonstrated its use for quantitative determination of irreversible deformations arising at testing steel against high-cycle fatigue, and assessed the associated measurement errors. The method allows reliably determining the relative displacements of the scattering centers of the surface to a value on the order of 10 nm with a base on the order of 10 μ m. In [14], it was shown that the method is superior against the available traditional methods of correlation and holographic interferometry by an order of magnitude, or even two orders of magnitude, in sensitivity and spatial resolution. In the above-mentioned works [12–14], the optical system allowed finding the projection of the relative displace-

ment vector of the surface points onto its normal. In addition, to localize the irreversible processes, the authors used samples with a Sharpy-type cut with a rounding at the cut apex of 0.25 mm. It was shown that there arises a zone of plastic deformation less than 1 mm in size in the course of crack initiation at the cut apex. In the current work, we used samples with a weak stress concentrator—namely, with two 2.5-mm-radius symmetrically placed grooves. In the course of fatigue testing of a sample, we first succeeded in determining not one, but three, components of the relative displacement vector on a small base on the order of 10 μ m. The work was mainly aimed at finding the limit values of the three components of the relative displacement vector of the surface points. Note that we can use various traditional optical [15–17] and nonoptical [1, 18–20] methods for studying the peculiarities of plastic deformations. However, there great methodological difficulties arise when we apply them for measurements at small bases.

Previously, in [13], we used the model of reflecting object as a combination of point scattering centers situated on its surface to solve the problem of the dynamics of speckles in the image plane of the periodically deformed object and derive the formulas for radiation intensity \tilde{I} in a point of the image plane and for the normed temporal auto-correlation function $\eta(t_1, t_2)$ of this intensity. We assumed that the value \tilde{I} is the time-averaged radiation intensity and the time of averaging takes the value of or is a multiple of period T of cyclic loads. For \tilde{I} , we obtained

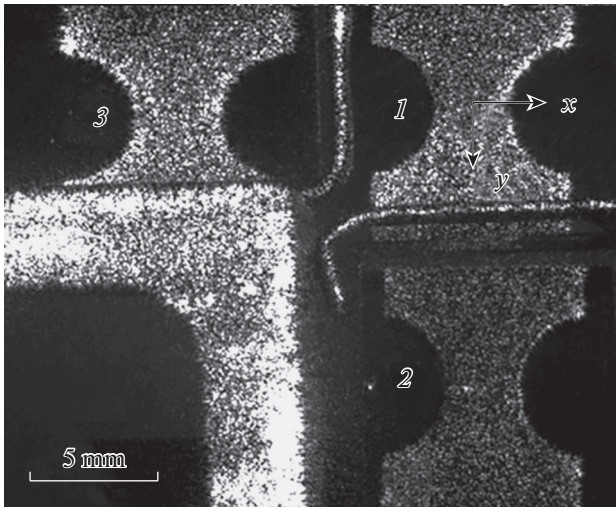


Fig. 1. Three speckle images (1–3) of a sample in one frame.

$$\tilde{I} = I_1 + I_2 \exp[-\sigma^2/2] \cos[x + \alpha], \quad (1)$$

$$\eta(t_1, t_2) = \eta_1 \eta_2 \eta_3 = \eta(u_x) \cos[\langle x_2 \rangle - \langle x_1 \rangle] \times \exp\left[-\frac{1}{2}k_{11} - \frac{1}{2}k_{22} + k_{12}\right]. \quad (2)$$

In formula (1), I_1 , I_2 , and α are constants; x and σ^2 is the mean value and the variance of the value $k\Delta\mathbf{u}(\mathbf{I}_s + \mathbf{I})$; $k = 2\pi/\lambda$ is the wavenumber; $\Delta\mathbf{u}$ is the relative displacement vector of two scattering centers located in the region with size Δy of the linear resolution of the lens; and \mathbf{I}_s and \mathbf{I} are the unit vectors directed from the region center to the light source and to the lens center, respectively. In formula (2), the function $\eta_1 = \eta(u_x)$ is the autocorrelation function corresponding to the translational motion of the object, where, for the sake of certainty, we have assumed that the object moves along the x axis; $\langle x_1 \rangle$ and $\langle x_2 \rangle$ are mean values; k_{11} and k_{22} are variances; k_{12} is the correlation moment of values x at time instances t_1 and t_2 , respectively; and the angular brackets denote the averaging over an ensemble of objects.

Figure 1 shows a typical frame with three speckle images of the planar working part of a sample with a thickness of 1.6 mm corresponding to three observation aspects. Image 1 was registered by the observation normal to the surface. Images 2 and 3 were generated with two identical prisms deviating the speckle-modulated waves scattered by the object towards the video camera objective lens. Roughness parameter Ra measured by a WYKO NT-1100 interference microscope was $0.8 \mu\text{m}$. Before and after fatigue testing of the sample, we recorded the three-dimensional profiles of the surface using the WYKO NT-1100 device. We cyclically loaded the samples on a RUMUL MIKROTRON high-frequency resonant testing stand

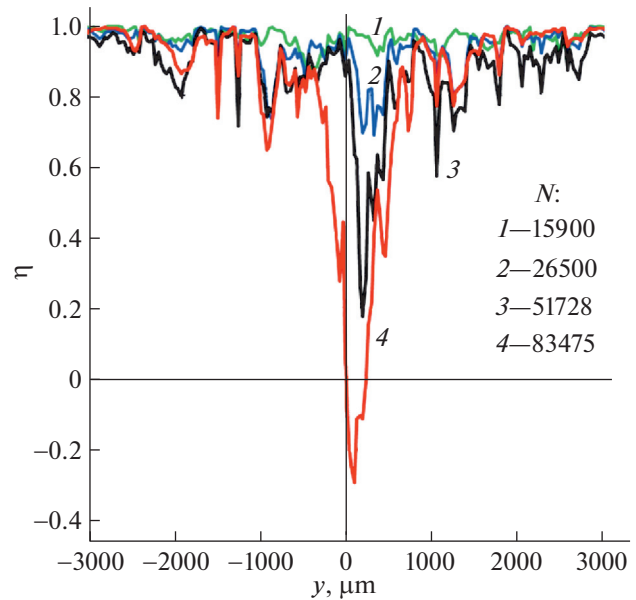


Fig. 2. Dependences $\eta(y)$ for different cycles $N(x \approx 3.0 \text{ mm})$.

using zero-to-tension cycling at a loading frequency of approximately 100 Hz and at a double amplitude of 2.0 kN. The sample was illuminated by a 20-mW laser module with wavelength $\lambda = 0.65 \mu\text{m}$. In this experiment, we used a VIDEOSKAN-415M-USB monochromatic video camera with a matrix comprising 782×582 photocells with a size of $8.3 \times 8.3 \mu\text{m}$. The averaging time of 0.5 s corresponded to 53 loading cycles. The dimensions of the video camera objective lens was selected so that the minimum size of speckles was somewhat larger than the size of a photocell in the camera photodetector matrix. The value of η on an image fragment with a size of $m \times m$ was determined by formula (38) from [13]. The original software recorded the current frames (that is, every 53 cycles of deformation) and the frames after each 1000 cycles of loading in separate files for their processing after the experiment. We stopped to test the samples when the resonance frequency varied by 10%.

Figure 2 depicts the distributions of value η along the vertical line on image 2 of the sample; the size of the image fragment is 5×5 pixels. The line passed through the region of speckle image corresponding to the segment of the surface near the cut, where a crack with a length on the order of $100 \mu\text{m}$ initiates at the end of our experiment. We see from the curves that the irreversible processes occur nonuniformly and there are local zones with increased values of plastic strain. Starting from approximately 30 thousand cycles, irreversible processes begin in one such zone, reducing value η to negative values. We found a crack in exactly this zone. Constructing a similar dependence $\eta(y)$ along the line passing through the segment corresponding to the sample center showed that the minimum value of η equal to 0.38 is achieved at one of the

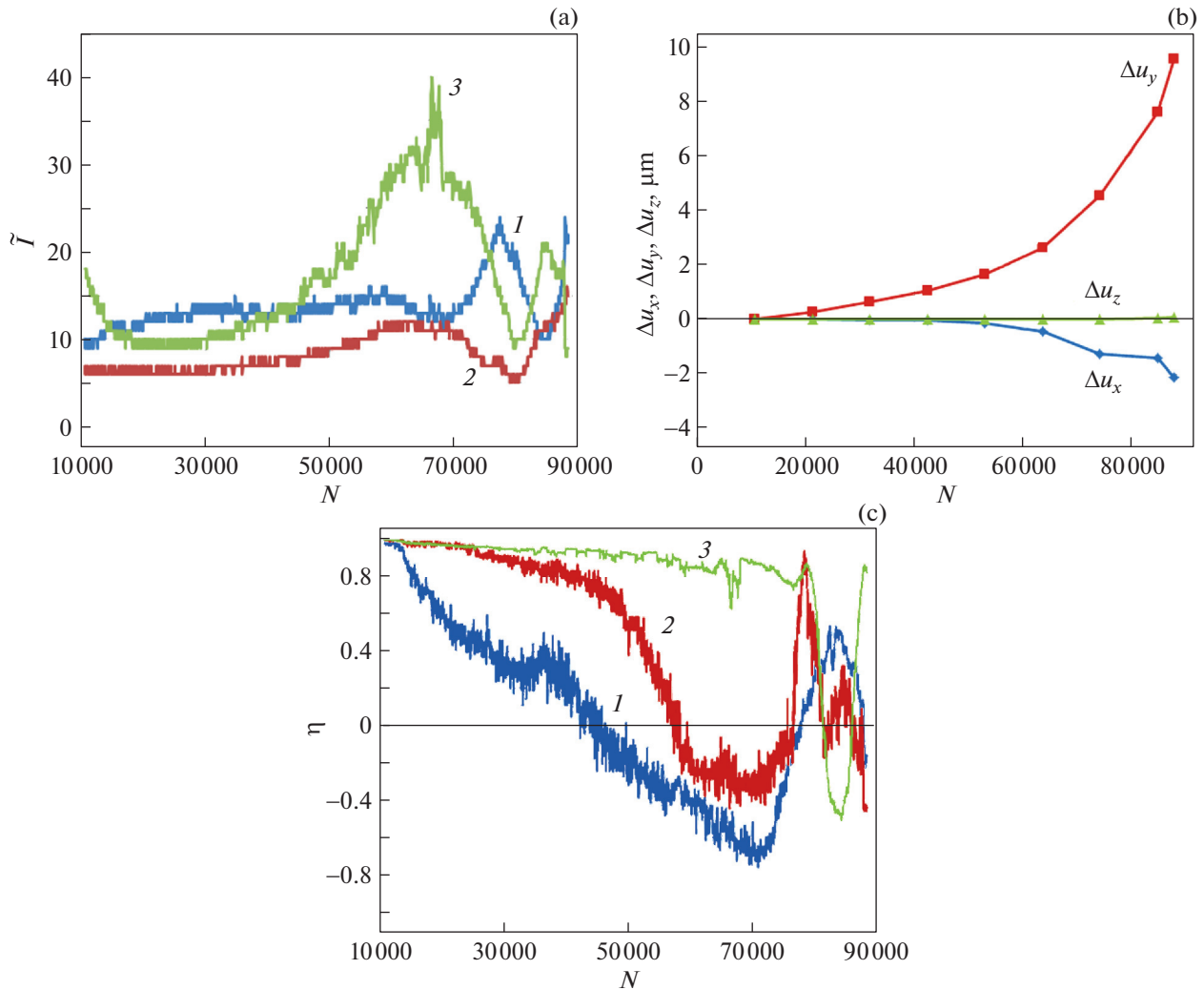


Fig. 3. (a) Dependences $\tilde{I}(N)$ for three aspects of observation (the curve indices corresponds to the indices of the sample images), (b) dependences of the components of vector $\Delta \mathbf{u}$ on number of cycles N , and (c) dependences of parameter η on number of cycles N (the curve indices correspond to the indices of the sample images).

localized deformation zones. In Fig. 3a, we present the dependences of digital radiation intensity value \tilde{I} on number of loading cycles N for three aspects of observation. The pixels on three images corresponded to the same region of crack initiation, namely, to the center of the zone of localized deformation. We see from the given curves that dependences $\tilde{I}(N)$ are quasi-periodic functions. According to formula (1), the maximum values of \tilde{I} correspond to the values of the cosine argument $x + \alpha$ equal to $\pm\pi n$ ($n = 1, 2, 3$). The minimum values of the curves correspond to the values of the argument equal to $\pm\pi(1 + 2n)$. For the three curves, we plotted the dependences of n on N ; all values were taken with a “+” sign. Experimental dependences $n(N)$ were approximated by the polynomials of third and fourth degree, and the approximation certainty was not less than 0.998. Afterwards, we divided

initial values n_0 from all values n and determined the values of the three values $\Delta n = n - n_0$ corresponding to the three directions of observation by using the known functions with a step of 10 thousand cycles. As a result of solving the three equations $\Delta \mathbf{u}(\mathbf{I}_s + \mathbf{I}) = \lambda \Delta n$ with experimentally known values of the components of the vectors \mathbf{I}_s and \mathbf{I} for each chosen cycle, we determined the three components Δu_x , Δu_y , and Δu_z of vector $\Delta \mathbf{u}$. In the equations we used the unit vector $\mathbf{I}_s(0, -0.190, 0.981)$, the unit vectors $\mathbf{I}(0, 0, 1)$, $\mathbf{I}(0, 0.310, 0.951)$, and $\mathbf{I}(0.308, 0, 0.982)$ corresponding to images 1, 2, and 3. In solving the system of equations, we took the sign of value Δn from the physical considerations, namely, from the condition that value Δu_z reaches its minimum value. Figure 3b illustrates the combined dependences of values Δu_x , Δu_y , and Δu_z on number of cycles N . We see that the maximum relative irreversible displacement of the surface points averaged both

in time and in the region with size $\Delta y = 66 \mu\text{m}$ tends to $10 \mu\text{m}$. Therefore, the limit tension plastic strain of the surface that we estimated as $\Delta u_y / \Delta y$ achieves a value on the order of 10^{-1} . Analyzing dependences $\eta(y)$ found with different values of N and $\eta(N)$ corresponding to different fragments of the image showed that it is appropriate to use the fact that value η is reduced to negative values as an indication of pre-fracture of a surface element. In Fig. 3c, we give dependences $\eta(N)$ corresponding to the zone of crack initiation for the three observation directions. The size of the fragment is 3×3 pixels. The above-mentioned curves imply that, by choosing the appropriate light and observation directions, we can register a reduction in η to zero at values N being 50% of the maximum value N equal to 89 thousand cycles. The found data may be a basis for creating physical models of high-cycle fatigue of materials and techniques for nondestructive diagnostics of the residual life of engineering parts. The limit value of the tension strain found in this work by order of value coincides with the limit strain arising at quasi-static tension tests of standard samples. This coincidence allows suggesting that the methods of nondestructive inspection, the techniques for assessing the damage of the objects by the methods of solid mechanics, and the methods of numerical evaluation of the stress–strain state of bodies developed for quasi-static loadings may be adapted for investigating the phenomena appearing at high-cycle fatigue of structural elements.

ACKNOWLEDGMENTS

The authors thank I.S. Kamantsev for aid in performing experiments.

FUNDING

The work was partially supported by Decree 211 of the Russian Government, agreement no. 02.A03.21.0006.

CONFLICT OF INTEREST

The authors declare that they have no conflicts of interest.

REFERENCES

1. D. A. Tupikin, *Kontrol' Diagn.*, No. 11, 53 (2003).
2. I. I. Novikov and V. A. Ermishin, *Physical Mechanics of Real Materials* (Nauka, Moscow, 2004) [in Russian].
3. J. Lasar, M. Hola, and O. Cip, in *Proceedings of the Conference Photo Mechanics* (Delft University, Netherlands, 2015), p. 64.
4. H. J. Gough, *The Fatigue of Metals* (E. Benn, London, 1926).
5. V. F. Terent'ev, *Fatigue of Metallic Materials* (Nauka, Moscow, 2002) [in Russian].
6. Y. Murakami, *Metal Fatigue: Effects of Small Defects and Nonmetallic Inclusions* (Academic, New York, 2019).
7. S. S. Manson, *Exp. Mech.* **5** (7), 193 (1965).
8. J. Schijve, *Int. J. Fatigue* **25**, 679 (2003).
9. R. Erf, *Holographic Nondestructive Testing* (Academic, New York, 1974).
10. E. Marom and R. K. Muller, *Int. J. Nondestruct. Test.* **3**, 171 (1971).
11. V. P. Kozubenko, V. A. Potichenko, and Yu. S. Borodin, *Probl. Prochn.*, No. 7, 103 (1989).
12. A. P. Vladimirov, I. S. Kamantsev, V. E. Veselova, E. S. Gorkunov, and S. V. Gladkovskii, *Tech. Phys.* **61**, 563 (2016).
13. A. P. Vladimirov, *Opt. Eng.* **55** (12), 1217 (2016).
14. A. P. Vladimirov, I. S. Kamantsev, N. A. Drukarenko, L. A. Akashev, and A. V. Druzhinin, *Opt. Spectrosc.* **127**, 943 (2019).
<https://doi.org/10.1134/S0030400X19110286>
15. L. B. Zuev, V. I. Danilov, and N. M. Mnikh, *Zavod. Lab.* **56** (2), 90 (1990).
16. M. A. Sutton, J.-J. Orteu, and H. Schreier, *Image Correlation for Shape, Motion and Deformation Measurements* (Univ. South Carolina, Columbia, USA, 2009).
17. S. V. Panin, P. S. Lyubutin, and V. V. Titkov, *Image Analysis in Optical Method of Deformation Assessment* (Sib. Otdel. RAN, Tomsk, 2017) [in Russian].
18. A. Gilanyi, K. Morishita, T. Sukegawa, M. Uesaka, and K. Miya, *Fusion Eng. Design* **42**, 485 (1998).
19. V. A. Ermishkin, D. P. Murat, and V. V. Podbel'skii, *Avtomatiz. Sovrem. Tekhnol.*, No. 2, 11 (2008).
20. O. A. Plekhov, I. A. Panteleev, and V. A. Leont'ev, *Fiz. Mezomekh.* **12** (5), 37 (2009).